Proceedings of the XII International Symposium on Dynamic Problems of Mechanics (DINAME 2007),
Varoto, P. S. and Trindade, M. A. (Editors), ABCM, Ilhabela, SP, Brazil, February 26 - March 2, 2007

Comparison between Unscented and Extended Kalman Filters for Nonlinear Aircraft Flight Path Reconstruction

Celso Braga de Mendonça[1] and Elder Moreira Hemerly[2]

[1] Empresa Brasileira de Aeronáutica – EMBRAER, Av. Faria Lima 2170, CEP 12227-900 São José dos Campos – SP, Brasil, celso.mendonca@embraer.com.br

[2] Technological Institute of Aeronautics – Electronics Division, Systems and Control Department, Praça Mal. Eduardo Gomes, 50 – Vila das Acácias, CEP12228-900 São José dos Campos/SP – Brazil, hemerly@ita.br

Abstract: Flight Path Reconstruction (FPR) is a technique applied to aircraft state and parameter identification to generate a consistent database, to be used in any subsequent application, commonly an aerodynamic stability and control derivative determination. This procedure assures consistency between flight data and aircraft kinematic equations. Air data sensors can also be calibrated simultaneously in a FPR scheme. Different procedures have been studied in the literature, even in a batch or a recursive data processing procedure, taking into account process and/or measurement noise. Among them, stochastic filtering is an attractive method because it considers process and measurement noise and can be used onboard during a flight test execution. Since a complete FPR model is a nonlinear problem, the Extended Kalman Filter (EKF) is usually adopted to handle the non-linear filtering problem. Nevertheless, one of the main drawbacks of the EKF is the linearization, which requires Jacobians evaluations and a sampling rate small enough not to violate linearization assumptions. More recently, other approaches have been proposed for nonlinear problems, such as the Unscented Kalman Filter (UKF). In this procedure state and covariance are propagated through some deterministically selected sigma points, instead of linearizing the models around the estimated trajectory. This paper compares the results obtained with the EKF and the UKF methods in the FPR problem, regarding consistency of the results, by using both simulated and flight test data.

Keywords: Flight Path Reconstruction, nonlinear systems, Extended Kalman Filter, Unscented Kaman Filter, Parameter Identification, flight test

NOMENCLATURE

A = dynamic matrix
E{} = expected value function
f = model dynamic function
H = observation matrix
h = measurement function
K = Kalman gain matrix
k = discrete time index
$\mathbf{P}_{xy}$ = covariance matrix between signals X and Y
Q = state noise covariance matrix
R = measurement noise cov. matrix
t = continuous time
k = discrete time
u = control vector
v = measurement noise vector
X = sigma point matrix
x = state vector
Y = transformed sigma point matrix
y = observation vector
z = measurement vector
W = process noise gain matrix
$\mathbf{W}_i^{(c,m)}$ = sigma points weighs
w = state noise vector

Greek Symbols

Φ = state transition matrix
Δt = sampling time
Θ = vector of unknowns
α, β, k = UKF parameters

Superscripts

T = transpose
-1 = matrix inverse
^ = estimated
- = predicted value
+ = corrected value

INTRODUCTION

Flight Path Reconstruction technique consists in checking the integrity and consistency of different sets of measurement data obtained in a flight test, relating them mathematically. During this process, states and their related calibration parameters are obtained simultaneously in a form that all measurement sets are made consistent among them considering measurements and models. Estimated states become a new corrected database to be used in any subsequent identification problems, for example, stability and control aerodynamic derivatives estimation. As a sub-product, air data estimated parameters consist also in the calibration parameters to be used by onboard by the air data computer.

The dynamic model used in a compatibility check analysis, normally in a space state form, comes from the aircraft kinematic equations. This model consists of a set of first order ordinary differential equations in which inputs have a mathematical rather then physical sense. Command surface inputs are replaced by specific forces and angular rates. An important aspect is that, using this approach, the inclusion of any aerodynamic and propulsion forces in the model is avoided. All formulations do not transport the inherent uncertainty of those estimates, which are complex to be determined and extracted from flight test data with a sufficient degree of confidence.

On-line analysis is an attempt to validate the test point before concluding the flight. This procedure provides a better efficiency and minimizes flight test repetitions. Laban [1] explored this approach using stochastic filtering. Recursive methods have adequate characteristics for on-line processing. His work got through the aerodynamic derivative determination using the two steps method. Mulder et al. [2] made a review of the flight path reconstruction methods and presented some new approaches for the problem. It was pointed out that better results would be obtained through the maximum likelihood method, but it did not show any advances regarding Laban's pure stochastic filtering approach. Laban [1] concluded that one of the practical difficulties associated with filtering methods is to choose properly process noise statistical properties.

The most common stochastic filtering method used in a FPR problem is the Extended Kalman Filter (EKF), which is an attempt to solve a nonlinear problem using standard Kalman filter equations. This is done by linearizing the nonlinear dynamic and output models along the estimated trajectory. This approximation is necessary to propagate states and variances and should be reliable enough to represent the nonlinear system. Linearization can be done only if Jacobian exists, but this does not hold in specific problems like those which involve discontinuities. Jacobian calculation should be done either analytically or numerically. While the first is error-prone for complex problems and particularizes the solution, the second requires a numerical procedure properly chosen to guaranty the desirable precision. An alternative method to treat the nonlinear stochastic filtering, the Unscented Kalman Filter (UKF), was proposed by Julier and Uhlmann [3] [4]. Its main idea is to approximate a Gaussian distribution, calculated after transforming some deterministically chosen points, instead of linearyzing a function. Some advantages are [3] [4]: i) avoid Jacobian calculation; ii) more realistic state variance estimation; iii) can be applied to non-differentiable functions; and iv) is valid for higher-order expansions rather than the standard EKF.

The main contribution of this work is to compare the EKF and the UKF methods in a Flight Path Reconstruction application. Both methods were implemented to run on-line in a flight test prototype as a single pass filter. As FPR problem is typically nonlinear the UKF would be more proper to handle this characteristic, nevertheless when the sampling rate is small enough the EKF linearization can be accurate enough. The effects of this tradeoff are analyzed in a true problem.

DEVELOPMENT

1. The Extended Kalman Filter

The dynamic and measurement mathematical model is assumed to be described by the following continuous-discrete stochastic equations

$$\begin{aligned} \dot{\mathbf{x}}(t) &= f(\mathbf{x}(t), \mathbf{u}(t), \mathbf{w}(t)) \\ \mathbf{y}(t) &= h(\mathbf{x}(t)) \\ \mathbf{z}(k) &= \mathbf{y}(k) + \mathbf{v}(k) \\ \mathbf{x}(0) &= \mathbf{x}0 \end{aligned} \tag{1}$$

Functions $\mathbf{f} \in \Re^n$ and $\mathbf{h} \in \Re^m$ are general nonlinear functions; vector $\mathbf{x} \in \Re^n$ is the state vector; $\mathbf{u} \in \Re^l$ is the input/control vector; $\mathbf{y} \in \Re^m$ is the output vector and $\mathbf{z} \in \Re^m$ is sampled at discrete points with a uniform Δt sampling time; vectors $\mathbf{w}$ and $\mathbf{v}$ are process and measurements stochastic noises respectively. Besides being modeled as stochastic variables, process noise terms also concentrate some deterministic dynamics from model approximations in practice, violating some initial assumptions. Noises are considered zero mean, white and with Gaussian distribution. They are also assumed to be independent between themselves and also with respect to the initial condition $\mathbf{x}(0)$, more precisely

$$\begin{aligned} &E\{\mathbf{w}(k)\} = 0; E\{\mathbf{v}(k)\} = 0 \\ &E\{\mathbf{w}(k)\mathbf{w}(j)^T\} = \mathbf{Q}\delta(k-j); E\{\mathbf{v}(k)\mathbf{v}(j)^T\} = \mathbf{R}\delta(k-j) \\ &E\{\mathbf{w}(k)\mathbf{v}(j)^T\} = 0; E\{\mathbf{x}(0)\mathbf{w}(k)^T\} = 0; E\{\mathbf{x}(0)\mathbf{v}(k)^T\} = 0 \end{aligned} \tag{2}$$

The standard Kalman filter addresses only linear stochastic systems and it is not directly applicable to nonlinear problems. On the other hand, there are no practical solutions for the general optimal nonlinear filtering problem. An artifice to use the Kalman filter equations in a nonlinear problem, with nonlinearities presented either in the dynamic or in the measurement model, is to linearize the system around the current state estimates. This approach is named Extended Kalman Filter (EKF). For this purpose a corresponding linear system is derived from the original one by calculating all necessary Jacobians. When model parameters are to be estimated simultaneously, a new state vector is then defined based on the previous state vector and on the proposed parameter vector, therefore resulting in the EKF augmented state vector.

The linearized system is calculated based on equation (1) through the following derivatives

$$\mathbf{A}(k) = \frac{\partial f(\mathbf{x}(t), \mathbf{u}(t), 0)}{\partial \mathbf{x}} \mid \hat{\mathbf{x}}(k)^+ ; \ \mathbf{W}(k) = \frac{\partial f(\mathbf{x}(t), \mathbf{u}(t), 0)}{\partial \mathbf{w}} \mid \hat{\mathbf{x}}(k)^+ ; \ \mathbf{H}(k) = \frac{\partial h(\mathbf{x}(t))}{\partial \mathbf{x}} \mid \hat{\mathbf{x}}(k)^- \tag{3}$$

With the Jacobians defined in equation (3), and calculating the transition matrix $\mathbf{\Phi} = e^{\mathbf{A}\Delta t}$, the standard Kalman filter equations can be used. The algorithm is divided in two steps [5] [6]: time propagation, and measurement correction. These steps are usually named as "prediction" and "correction" respectively. Initial state $\hat{\mathbf{x}}(0)$ and covariance matrix $\mathbf{P}(0)$ are assumed at first and then are propagated using

$$\begin{aligned} \hat{\mathbf{x}}^-(k+1) &= \hat{\mathbf{x}}^+(k) + \int_{t_k}^{t_{k+1}} f(\mathbf{x}(t), \mathbf{u}(t), 0) dt \\ \mathbf{P}^-(k+1) &\approx \mathbf{\Phi}_{k,k+1} \mathbf{P}^+(k) \mathbf{\Phi}_{k,k+1}{}^T + \mathbf{W}(k+1)^T \mathbf{Q}(k) \mathbf{W}(k+1) \end{aligned} \tag{4}$$

The propagation is done until more information is available from the sensors and can be incorporated in the filter. This is the correction phase and it updates, based on the Kalman gain matrix and on the innovations, states and covariances as

$$\begin{aligned} \mathbf{K}(k) &= \mathbf{P}^-(k)\mathbf{H}^T(\mathbf{H}\mathbf{P}^-(k)\mathbf{H}^T + \mathbf{R}(k))^{-1} \\ \hat{\mathbf{x}}^+(k) &= \hat{\mathbf{x}}^-(k) + \mathbf{K}(k)(\mathbf{z}(k) - \mathbf{H}\hat{\mathbf{x}}^-(k)) \\ \mathbf{P}^+(k) &= (\mathbf{I} - \mathbf{K}(k)\mathbf{H})\mathbf{P}^-(k) \end{aligned} \tag{5}$$

In the next section the Unscented Kalman Filter algorithm is summarized.

2. The Unscented Kalman Filter

The Unscented Kalman Filter was developed by Julier e Uhlmann [3] [4]. Its main idea is to approximate a probability distribution instead of approximating a general nonlinear function using a linearization process. This is done choosing a deterministically set of points, called sigma points, which capture current mean and covariance filter estimates. A nonlinear transformation is applied to these points generating a new set of transformed sample. There are no restrictions about the actual distribution and a Gaussian distribution can be approximated by calculating the predicted mean and covariance based on this transformed data set. Using this procedure it is not necessary to calculate Jacobians. The method is described in details in references [3] [4], and here only the algorithm is presented.

Given the estimated state vector $\mathbf{x}(k\text{-}1)^+$, a set of sigma point vectors $(\mathbf{X}(k\text{-}1))_i$ can be calculated as

$$(\mathbf{X}(k-1))_0 = \hat{\mathbf{x}}(k-1) \tag{6}$$

$$(\mathbf{X}(k-1))_i = \hat{\mathbf{x}}(k-1) + (\sqrt{(n+\lambda)\mathbf{P}(k-1)})_i, \ i = 1,\ldots,n \tag{7}$$

$$(\mathbf{X}(k-1))_i = \hat{\mathbf{x}}(k-1) - (\sqrt{(n+\lambda)\mathbf{P}(k-1)})_{i-n}, \ i = n+1,..,2n \tag{8}$$

where $(\sqrt{(n+\lambda)P(k-1)})_i$ is the *ith* column of a matrix square root. Since the full matrix is positive definite, a Cholesky decomposition can be used to calculate this term. The constant λ is defined as

$$\lambda = \alpha^2 (n+k) - n \tag{9}$$

where α and k are design parameters that define the spread of the sigma points.

After the sigma point matrix **X**(k-1) is calculated the prediction step is carried out by integrating each column, using the dynamic model **f**(x) and a 4th order Runge Kutta method, for example. The propagated matrix becomes

$$\mathbf{X}(k)_i = f(X(k-1)_i)\text{ , i = 0,…,2n} \tag{10}$$

State predicted values can be obtained based on each column of matrix ***X***(k) as

$$\hat{\mathbf{x}}(k)^- = \sum_{i=0}^{2n} W_i^m (\mathbf{X}(k))_i \tag{11}$$

where the weighs values W_i^m are calculated as

$$W_0^m = \frac{\lambda}{(n+\lambda)}\text{, and } W_i^m = \frac{1}{2(n+\lambda)}\text{, i = 1,…,2n} \tag{12}$$

The predicted covariance matrix is calculated as

$$\mathbf{P}(k)^- = \sum_{i=0}^{2n} W_i^c (\mathbf{X}(k)_i - \hat{\mathbf{x}}(k)^-)(\mathbf{X}(k)_i - \hat{\mathbf{x}}(k)^-)^T + \mathbf{Q}(k) \tag{13}$$

It was considered an additive process noise vector, otherwise the process noise covariance matrix term **Q**(k) vanish in equation (13) and the state vector should be augmented by the noise terms. The weights constants are defined by

$$W_0^c = \frac{\lambda}{(n+\lambda)} + (1-\alpha^2+\beta)\text{, and } W_i^c = \frac{1}{2(n+\lambda)}\text{, i = 1,…,2n} \tag{14}$$

where β is a design parameter which incorporates prior knowledge about the distribution of the state vector. Once computed the predicted states, the predicted output vector is calculated using the measurement model, i.e.,

$$\mathbf{Y}(k)_i = h(\mathbf{X}(k)_i)\text{ , i = 0,…,2n} \tag{15}$$

and

$$\hat{\mathbf{y}}(k)^- = \sum_{0}^{2n} W_i^m (\mathbf{Y}(k))_i \tag{16}$$

The Kalman gain needs to be calculate to perform the correction step using the definition, via

$$\mathbf{K}(k) = \mathbf{P}(k)_{XY}\, \mathbf{P}(k)_{YY}^{-1} \tag{17}$$

where

$$\mathbf{P}(k)_{YY} = \sum_{i=0}^{2n} W_i^c (\mathbf{Y}(k)_i - \hat{\mathbf{y}}(k)^-)(\mathbf{Y}(k)_i - \hat{\mathbf{y}}(k)^-)^T + \mathbf{R}(k) \tag{18}$$

and

$$\mathbf{P}(k)_{XY} = \sum_{i=0}^{2n} W_i^c (\mathbf{X}(k)_i - \hat{\mathbf{x}}(k)^-)(\mathbf{Y}(k)_i - \hat{\mathbf{y}}(k)^-)^T \tag{19}$$

The same comments made to process noise covariance matrix hold for the measurement noise covariance matrix **R**(k) in equation (18).

Concluding the correction step, the corrected state vector and covariance matrix are computed as

$$\hat{\mathbf{x}}(k)^+ = \hat{\mathbf{x}}(k)^- + \mathbf{K}(k)(\mathbf{z}(k) - \hat{\mathbf{y}}(k)^-) \tag{20}$$

and

$$\mathbf{P}(k)^+ = \mathbf{P}(k)^- - \mathbf{K}(k)\mathbf{P}(k)_{YY}\mathbf{K}(k)^T \tag{21}$$

3. Flight Path Reconstruction Formulation

Four groups of first order differential equations, generally represented in a space state form, are necessary to characterize the aircraft motion. Newton's Law is applied in a rotating aircraft body fixed referential system – considering the Earth as flat and as an inertial reference frame. A kinematic model can be derived by substituting traditional physical inputs by measured variables, such as specific aerodynamic forces, which mean a summation of all aerodynamic and propulsion forces divided by aircraft mass, and body rotational rates. Specific forces can be measured by typical accelerometers, preferentially installed in the center of gravity and aligned with body reference frame. Among these four set of equations, only the rotational equations of motion are not used in a FPR problem. Airspeed information is included in the model through static and total pressure measurements. It is possible to establish a dynamic behavior for the static pressure, and relate it to other state variables, assuming the air as a dry and perfect gas [9]. All constant parameters are modeled as random walk to allow adequate variation from initial conditions, to avoid the associated state error covariance convergence to zero and because the time invariance assumption is not fully correct. These equations will just be presented here and other works [7] [8] [9] should be sought for details. The dynamic model is then summarized as

$$\begin{aligned}
\dot{u} &= (ax_{cg} + b_{ax} + wp_{ax}) - ((q_m + b_q + wp_q)w - (r_m + b_r + wp_r)v) - g sen\ \theta \\
\dot{v} &= (ay_{cg} + b_{ay} + wp_{ay}) - ((r_m + b_r + wp_r)u - (p_m + b_p + wp_p)w) + g\cos\theta sen\ \phi \\
\dot{w} &= (az_{cg} + b_{az} + wp_{az}) - ((p_m + b_p + wp_p)v - (q_m + b_q + wp_q)u) + g\cos\theta\cos\phi \\
\dot{\phi} &= (p_m + b_p + wp_p) + (q_m + b_q + wp_q) sen\ \phi \tan\theta + (r_m + b_r + wp_r)\cos\phi\tan\theta \\
\dot{\theta} &= (q_m + b_q + wp_q)\cos\phi - (r_m + b_r + wp_r) sen\ \phi \\
\dot{\psi} &= (q_m + b_q + wp_q) sen\ \phi \sec\theta + (r_m + b_r + wp_r)\cos\phi\sec\theta \\
\begin{bmatrix} \dot{x}_E \\ \dot{y}_E \\ -\dot{h}_E \end{bmatrix} &= L_{EB} \begin{bmatrix} u \\ v \\ w \end{bmatrix} \\
\dot{W}_N &= wp_{W_N};\ \dot{W}_E = wp_{W_E};\ \dot{W}_Z = wp_{W_Z} \\
\dot{P}s &= -\frac{Ps.g}{R.SAT}((sen\ \theta)u - (sen\ \phi\cos\theta)v - (\cos\phi\cos\theta)w) + wp_{Ps} \\
\dot{b}_{ax} &= wp_{bax};\ \dot{b}_{ay} = wp_{bay};\ \dot{b}_{az} = wp_{baz} \\
\dot{b}_p &= wp_{bp};\ \dot{b}_q = wp_{bq};\ \dot{b}_r = wp_{br} \\
\dot{K}_\alpha &= wp_{K\alpha};\ \dot{b}_\alpha = wp_{b\alpha} \\
\dot{K}_\beta &= wp_{K\beta};\ \dot{b}_\beta = wp_{b\beta} \\
\dot{K}_{Ps} &= wp_{KPs};\ \dot{b}_{Ps} = wp_{bPs}
\end{aligned} \tag{22}$$

The extended state vector is

$$\mathbf{x} = [\ u\ v\ w\ \phi\ \theta\ \psi\ xE\ xE\ hE\ WN\ WE\ WZ\ Ps\ bax\ bay\ baz\ bp\ bq\ br\ K\alpha\ b\alpha\ K\beta\ b\beta\ KPs\ bPs\ ],\ \epsilon\ \Re^{25} \tag{23}$$

and the process noise vector is

$$\mathbf{w} = [\ \text{wpax wpay wpaz wpp wpq wpr wpW}_N\ \text{wpW}_E\ \text{wpWz wpPs wpbax wpbay} \ldots$$

$$\text{wpbaz wpbp wpbq wpbr wpK}\alpha\ \text{wpb}\alpha\ \text{wpK}\beta\ \text{wpb}\beta\ \text{wpKPs wpbPs }],\ \epsilon\ \Re^{22} \tag{24}$$

Measurement error sources could be analyzed individually in detail. Therefore there is a general formulation that fits well for most of the typical flight test data cases [10], including air data calibration. As an example, by using this framework for the longitudinal specific force measurement, its calibration formula is

$$a_{xm} = K_{ax} a_x (t - \tau_{ax}) + b_{ax} + wm_{ax} \tag{25}$$

This model contains a scale factor K_{ax}, a bias term b_{ax}, a time delay term τ_{ax} and an additive measurement noise wm_{ax}. The measured variable is represented by the left side with the subscript *m*.

In this work the time delay is not considered and other simplifications were adopted according to each sensor characteristic. Bias term is preserved to compensate for cumulative integration errors, when required.

The output vector was chosen considering the sensor set available and to guarantee system observability. The sensors chosen for this work are: i) angle of attack probe; ii) sideslip vane; iii) static pressure probe, conjugated with the angle of attack probe; iv) Kiel Pitot for total pressure measurement; and v) GPS receiver for position determination. Thus, the measurement model is designed based on a simplified version of equation (25), leading to

$$\begin{aligned}
&\alpha m = K_\alpha tg^{-1}\left(\frac{w_a - x_\alpha q + y_\alpha p}{u_a}\right) + b_\alpha + wm_\alpha \\
&\beta m = K_\beta tg^{-1}\left(\frac{v_a + x_\beta r - z_\beta p}{u_a}\right) + b_\beta + wm_\beta \\
&Psm = Ps\left[1 + K_{Ps}\left(\left(\frac{7.R.SAT + V^2}{7.R.SAT}\right)^{7/2} - 1\right)\right] + \frac{Ps.g}{R.SAT}\begin{bmatrix}(x_{Ps} - x_{CG})sen(\theta) \\ -(z_{Ps} - z_{CG})\cos(\theta)\end{bmatrix} + b_{Ps} + wm_p \\
&Ptm = Ps\left[1 + \frac{V^2}{7.R.SAT}\right]^{7/2} + \frac{Ps.g}{R.SAT}\left[(x_{Ps} - x_{CG})sen(\theta) - (z_{Ps} - z_{CG})\cos(\theta)\right] \\
&+ \frac{Ps.V}{R.SAT}\left[(y_{Pt} - y_{CG})r - (z_{Pt} - z_{CG})q\right] + wm_{Pt} \\
&x_E m = x_E + wm_{xE} \\
&y_E m = y_E + wm_{yE} \\
&z_E m = z_E + wm_{zE}
\end{aligned} \tag{26}$$

In equation (26) all x_i, y_i and z_i which appear in the first fourth equations are sensor coordinate positions related to aircraft center of gravity. The aerodynamic speeds u_a, v_a and w_a are obtained from a subtraction between the inertial speed and the wind speed vectors. Terms K_i and b_i are scale factor and bias respectively. Based on equation (26), the output vector is given by

$$\mathbf{y} = [\ \alpha\text{m}\ \beta\text{m Psm Ptm xEm yEm zEm }],\ \epsilon\ \Re^7 \tag{27}$$

and the parameter vector is

$$\mathbf{\Theta} = [\ \text{bax bay baz bp bq br K}\alpha\ \text{b}\alpha\ \text{K}\beta\ \text{b}\beta\ \text{KPs bPs }],\ \epsilon\ \Re^{12} \tag{28}$$

The measurement noise vector assumes the form

$$\mathbf{v} = [\ \text{wm}\alpha\ \text{wm}\beta\ \text{wmPs wmPt wmxE wmyE wmhE }],\ \epsilon\ \Re^7 \tag{29}$$

DATA ANALYSIS

In this section a comparison between the EKF and the UKF methods is done in a flight path reconstruction application using simulated data, generated through a fixed base simulator, and flight test data obtained from a typical regional jet prototype flight test.

1. Simulated Data

The maneuver chosen to evaluate state and parameter estimation, in a sense of flight path reconstruction and simultaneous air data calibration, is the well known wind box [9]. This maneuver provides enough information for this purpose using angle off attack and angle of sideslip sweeps and speed variations. Its horizontal profile is characterized in figure 1. Simulated data was corrupted by process and measurement noise with typical signal to noise levels found in real applications. It was also included bias and scale factor errors in angle of attack, angle of sideslip and static pressure measurements. A sampling rate of 0.1s was adopted, which is considered a poor lower bound for identification purposes regarding this kind of application. The UKF parameters chosen was $\alpha = 1$, $\beta = 2$, and $k = 0$ [4]. Another EKF and UKF design parameters are the **R** and **Q** matrix. While the first was calculated through existing time histories, the second was adjusted based on residuals and theoretical innovation bounds analysis and by comparing the results with the known simulated values [9]. The same matrixes were adopted for both UKF and EKF methods.

A low sampling rate could violate the conditions necessary to linearize the model along the estimated trajectory, required in the EKF algorithm. Nevertheless a comparison of EKF and UKF estimated time histories, presented in figures 2, figure 3 and figure 4, show no significant differences between both results. Although other results are available, only those related to angle of attack are presented for conciseness and because they lead to the same conclusions. In figure 2 angle of attack estimates by both methods, curves blue and cyan, based on wind and inertial speeds states, are practically coincident. The same happens even for the prediction, which means how the output equations explain the measurements, curves in yellow and green. Figure 3 depicts the time histories of the angle of attack calibration parameters. Only a small difference is observed in the final value for the bias term. Finally figure 4 exhibits alpha calibration parameters variance, and again no visible difference is observed.

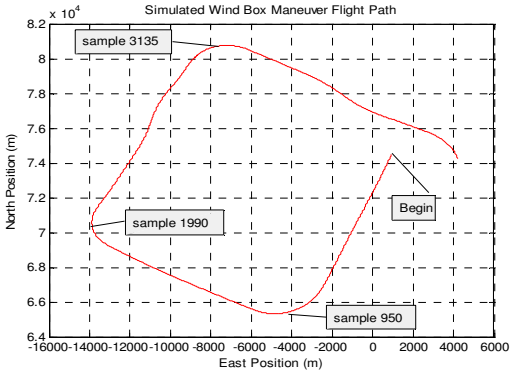

Figure 1 – Simulated flight path.

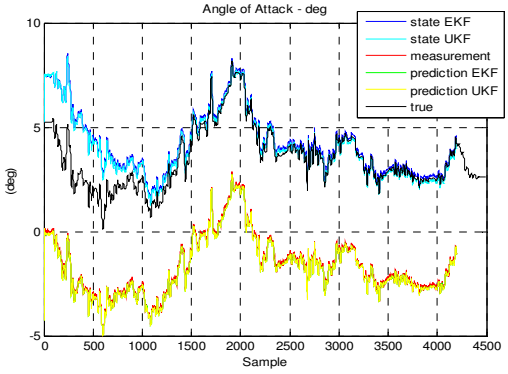

Figure 2 – Alfa time histories.

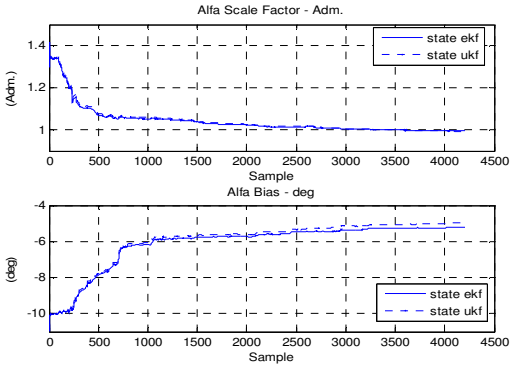

Figure 3 – Alfa calibration parameters.

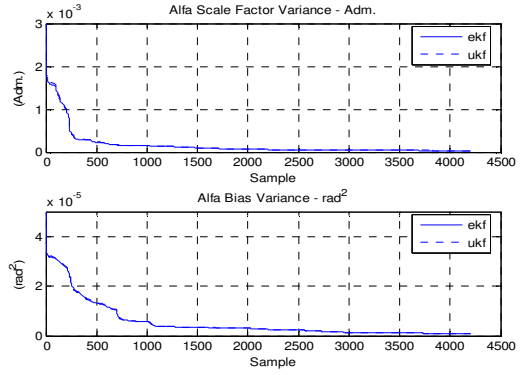

Figure 4 – Alfa Calibration parameters variance.

All parameter values were obtained through the mean of the last 400 samples of the respective estimated states. A comparison between true values and the estimated ones using both methods is shown in table 1.

Table 1 – Comparison of the estimated calibration parameters by the EKF and the UKF methods with simulated data.

	True	EKF	Error (%)	UKF	Error(%)
Alfa Scale Factor	0.95	0.995	4.7%	0.9945	4.7%
Alfa Bias (deg)	-5	-5.2392	4.8%	-4.9999	0.0%
Beta Scale Factor	0.95	0.9499	0.0%	0.9584	0.9%
Beta Bias (deg)	2	1.9088	-4.6%	1.8914	-5.4%
Static Pressure Scale Factor	0	0.0013	-	0.0013	-
Static Pressure Bias (Pa)	500	505.3053	1.1%	505.8184	1.2%

A comparison between estimated variances, calculated as a mean of the last 400 values, for the EKF and the UKF is made in table 2.

Table 2 – Comparison of the estimated state variances by the EKF and the UKF methods with simulated data.

State	Unit	Variance EKF	Variance UKF	Difference based on the EKF (%)
u	m/s^2	7.59E-04	8.12E-04	6.9%
v	m/s^2	2.63E-02	2.79E-02	6.1%
w	m/s^2	3.34E-02	3.49E-02	4.5%
phi	deg^2	5.84E-06	5.70E-06	-2.4%
theta	deg^2	2.20E-06	2.28E-06	3.5%
psi	deg^2	1.56E-06	1.65E-06	5.9%
x	m^2	3.15E-04	3.17E-04	0.4%
y	m^2	2.74E-04	2.77E-04	1.1%
h	m^2	3.20E-04	3.20E-04	0.0%
Wn	m/s^2	4.40E-03	4.40E-03	0.0%
We	m/s^2	2.60E-03	2.60E-03	0.0%
Wu	m/s^2	2.51E-02	2.49E-02	-0.8%
psi	Pa^2	1.05E+01	1.05E+01	0.2%
bax	m/s^2^2	1.14E-04	1.13E-04	-0.8%
bay	m/s^2^2	2.10E-04	2.05E-04	-2.3%
baz	m/s^2^2	3.20E-06	3.14E-06	-1.6%
p	rad/s^2	2.73E-09	2.73E-09	0.0%
q	rad/s^2	2.71E-09	2.71E-09	-0.1%
r	rad/s^2	2.59E-09	2.59E-09	0.0%
Ka	Adm	4.16E-05	4.22E-05	1.4%
ba	deg^2	1.02E-06	1.01E-06	-1.0%
Kb	Adm	2.00E-05	2.06E-05	3.1%
bb	deg^2	7.25E-07	7.42E-07	2.4%
KPs	Adm	3.99E-09	3.99E-09	-0.1%
bPs	Pa^2	1.09E+01	1.09E+01	0.2%

Julier and Uhlmann [3] pointed out that one of the main drawbacks of the Extended Kalman filter is that sometimes the algorithm estimates unrealistic state variances, which become excessively small. This behavior was not observed in this analysis and both methods presented similar results.

2. Flight Test Data

For performance comparison with real data, a regional jet instrumented prototype was used to generate all data necessary for the analysis. Instead of a wind box maneuver, it was selected a condensed one which contains angle of attack and angle of sideslip excursions followed by an 180^{o} turn. This trajectory is presented in figure 5. Although there are no true values to be compared with, filters results are confronted against a calibrated data based on a reference method proposed by Olson [11]. This method has some shortcomings because it requires special flight conditions – low turbulence level, constant horizontal wind and no vertical wind– as well as special instrumentation. A sampling rate of 0.015s was adopted and the UKF design parameters were the same adopted by the simulated case. The same **R** and **Q** matrix used in the simulated case were adopted for the flight data analysis.

The results obtained with real flight data were similar to those obtained with simulated data, as presented in figures 5 to 8. No significant difference between both methods is evident except for a small disagreement in the initial samples in figure 6 and figure 7. It seems that at the beginning the UKF estimated states are closer to the true values than the EKF estimates. But, as long as the parameters and states converge, and the estimated trajectory becomes more realistic, the UKF and EKF estimates assume similar values.

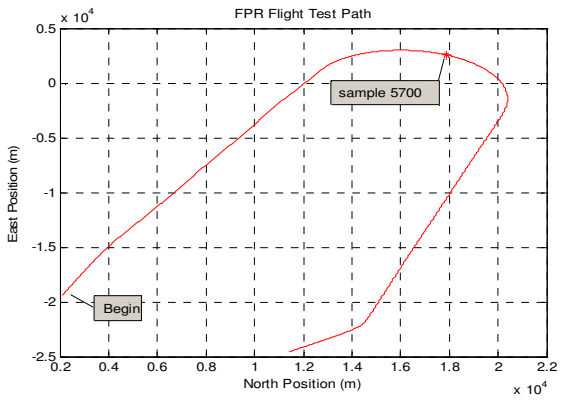

Figure 5 – Aircraft flight path.

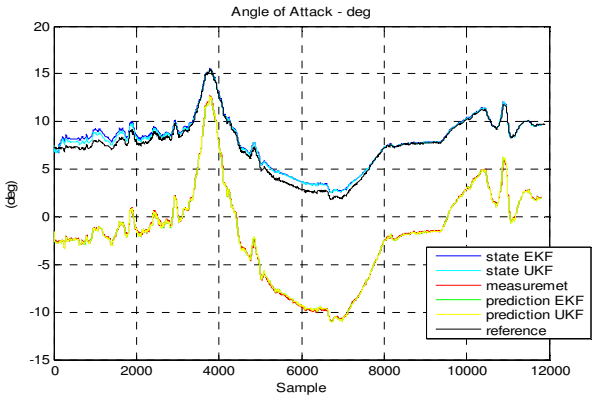

Figure 6 – Alfa time histories.

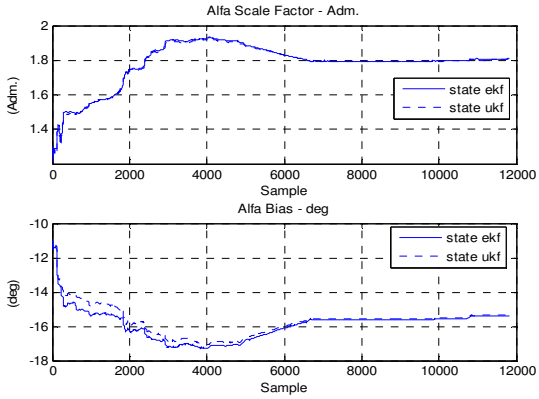

Figure 7 – Alfa calibration parameters.

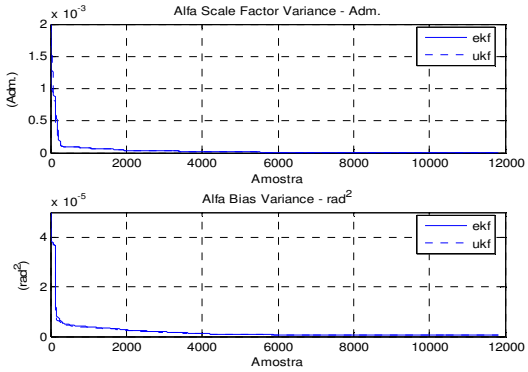

Figure 8 – Alfa Calibration parameters variance.

Estimated variances are compared in table 3 and again both methods presented similar results. Table 4 compares estimated calibration parameter for angle of attack and angle of sideslip against the reference method.

Table 3 – Comparison of the estimated state variances by the EKF and the UKF methods with flight test data.

State	Unit	Variance EKF	Variance UKF	Difference based on the EKF (%)
u	m/s^2	2.69E-04	2.73E-04	1.4%
v	m/s^2	7.20E-03	7.20E-03	0.0%
w	m/s^2	3.00E-03	3.10E-03	3.3%
phi	deg^2	9.47E-07	9.48E-07	0.1%
theta	deg^2	3.53E-07	3.51E-07	-0.6%
psi	deg^2	8.14E-07	8.08E-07	-0.6%
x	m^2	6.47E-05	6.51E-05	0.6%
y	m^2	1.61E-04	1.62E-04	0.6%
h	m^2	4.88E-06	4.97E-06	1.7%
Wn	m/s^2	3.10E-03	3.10E-03	0.0%
We	m/s^2	6.00E-03	6.00E-03	0.0%
Wu	m/s^2	4.40E-03	4.40E-03	0.0%
psi	Pa^2	1.38E+01	1.48E+01	7.4%
bax	m/s^2^2	2.92E-05	2.90E-05	-0.8%
bay	m/s^2^2	3.00E-05	3.01E-05	0.6%
baz	m/s^2^2	5.16E-06	5.16E-06	-0.1%
p	rad/s^2	6.26E-11	6.25E-11	-0.2%
q	rad/s^2	5.16E-11	5.17E-11	0.1%
r	rad/s^2	5.39E-11	5.41E-11	0.2%
Ka	Adm	7.66E-06	7.59E-06	-1.0%
ba	deg^2	4.45E-07	4.30E-07	-3.4%
Kb	Adm	2.43E-06	2.47E-06	1.9%
bb	deg^2	2.83E-07	2.72E-07	-3.6%
KPs	Adm	9.16E-07	9.10E-07	-0.6%
bPs	Pa^2	3.40E+01	3.40E+01	0.0%

Table 4 – Comparison of the estimated calibration parameters by the EKF and the UKF methods with flight test data.

	Reference	EKF	Difference (%)	UKF	Difference (%)
Alfa Scale Factor	1.84	1.805	-1.9%	1.8025	-2.0%
Alfa Bias (deg)	-14.8	-15.3976	4.0%	-15.3516	3.7%
Beta Scale Factor	1.55	1.4882	-4.0%	1.4893	-3.9%
Beta Bias (deg)	0.43	0.5237	21.8%	0.4842	12.6%

An analysis over the results shown in Tables 3 and 4 The UKF results are a little closer to the reference but both EKF and UKF results are similar.

CONCLUSION

The FPR application is essentially a nonlinear problem and the EKF has been extensively applied in its solution. The method has some shortcomings because requires Jacobian calculations to linearize the models and an appropriate sampling rate not to violate linearization assumptions. The UKF has been presented as an alternative method to solve nonlinear stochastic filtering problems and has some advantages over the EKF because does not requires Jacobians calculation, instead, approximates Gaussian distributions propagating some deterministically selected point, the sigma points.

In this paper it was made a comparison between the Extended Kalman Filter and the Unscented Kalman Filter applied to a Flight Path Reconstruction and simultaneous air data calibration application. Both methods were tested with simulated data and real flight test data.

Both filter performance were good and no essential difference between the results were observed. It is proposed, as an extension of this work, to evaluate the influence of lower sampling rates over the results using the EKF and the UKF.

REFERENCES

[1] Laban, M. – "On-Line Aircraft Aerodynamic Model Identification". PhD Dissertation, Delft University of Technology, Delft, The Netherlands, 1994.

[2] Mulder, J. A. et al. – "Non-linear Aircraft Flight Path Reconstruction Review and New Advances". Progress in Aerospace Sciences, No. 35, 1999, pp. 673-726.

[3] Julier, Simon J., Jeffery K. Uhlmann, and Hugh F. Durrant-Whyte. A New Approach for Filtering Nonlinear Systems.In Proceedings of the 1995 American Control Conference, 1628-1632, 1995.

[4] Julier, S. J. and Uhlmann, J. K. (2004). Unscented filtering and nonlinear estimation. Proceedings of the IEEE, 92(3):401–422.

[5] Gelb, A. – "Applied Optimal Estimation". MIT Press, Massachusetts, 1974.

[6] Kalman, R. E. – "A New Approach to Linear Filtering and Prediction Problems". Transaction of the ASME – Journal of Basic Engineering, pp. 35-45, 1960.

[7] Mendonça, C. B., Hemerly, E. M. e Góes, L. C. S. – "Calibração Anemométrica e Reconstrução de Trajetória de Aeronaves Utilizando Filtro de Kalman Estendido", CBA2006, XVI Congresso Brasileiro de Automática, Salvador-BA, 2006.

[8] Mendonça, C. B. , Hemerly, E. M. e Curvo, M. – "Reconstrução de Trajetória de Aeronaves com Identificação Paramétrica em Modelo Não-Linear", CBA2004, XV Congresso Brasileiro de Automática, Gramado-RS, 2004.

[9] Mendonça, C.B. – "Análise de Compatibilidade de Dados de Ensaio em Vôo e Calibração dos Dados do Ar em Tempo Real com Filtragem Estocástica Adaptativa". Tese de Doutorado, Instituto Tecnológico de aeronáutica, ITA, São José dos Campos, São Paulo, 2005.

[10] Jategaonkar, R. V. – "Short Course in Conjunction with DINCON-2003", ITA/CTA, São José dos Campos, Brazil, August, 2003.

[11] Olson, M. W. – "Aircraft Performance Flight Testing". Air Force Flight Test Center, Edwards Air Force Base, California, February 2003.

RESPONSIBILITY NOTICE

The author(s) is (are) the only responsible for the printed material included in this paper.